ACS OMEGA

Open Access

http://pubs.acs.org/journal/acsodf

Article

Adsorptive Removal of Cd(II) Ions from Water by a Cheap Lignocellulosic Adsorbent and Its Reuse as a Catalyst for the Decontamination of Sulfamethoxazole

Opeoluwa I. Adeiga and Kriveshini Pillay*

Cite This: *ACS Omega* 2024, 9, 38348−38358

Read Online

ACCESS | Metrics & More | Article Recommendations | Supporting Information

ABSTRACT: The work reports the removal of cadmium from water by applying an efficient low-cost lignocellulosic adsorbent, rooibos tea waste. The cadmium-loaded rooibos tea waste was used for the photocatalytic abatement of sulfamethoxazole to cater to the setback of secondary pollution mostly associated with the adsorption technique. The rooibos tea waste adsorbent displayed a high removal efficiency of about 90.63% for 10 mg/L Cd(II) ions at 45 °C, 180 min agitation time, pH 7, and a dosage of 500 mg. The process of Cd(II) adsorption was endothermic and spontaneous. Also, the spent adsorbent was found to be efficient toward the photocatalytic breakdown of 10 mg/L sulfamethoxazole with a degradation efficiency of 69% after 150 min. In addition, the extent of mineralization of the sulfamethoxazole by the spent adsorbent as obtained from the total organic carbon data was found to be 53%. Therefore, based on the results obtained from this work, rooibos tea waste lends itself as a cheap, eco-friendly, easily sourced, and viable adsorbent for the removal of toxic ions like Cd(II). Also, the successful reuse of the spent adsorbent is a promising approach to cater to the major setback of secondary pollution associated with adsorption technology.

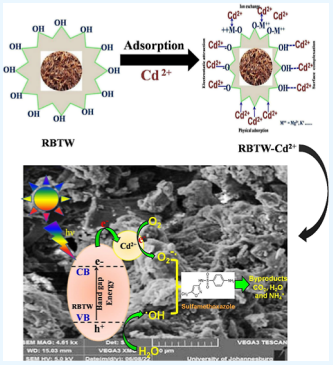

1. INTRODUCTION

Pollution arising from highly toxic metal ions, such as cadmium, continues to pose a great challenge globally.[1] This can be attributed to the exponential rise in industrialization and urbanization.[2] As a result of industrial activities associated with mines, paints, electroplating, plastics, fertilizers, pesticides, cadmium−nickel battery-producing factories, and so on,[3,4] cadmium finds its way into the ecosystem, thereby constituting a great risk to the health of human beings and aquatic life.[5] Cadmium(II) ions are generally known to be nonbiodegradable and persistent. Also, as a result of their long half-life, they are not easily metabolized when present in the human body, thus they can easily be concentrated in some organs such as the kidney and liver.[6,7] Cadmium has been reported to be one of the most hazardous and deadly trace metals owing to its toxicity and carcinogenicity even at a very low concentration.[8] Water containing cadmium ions if consumed can inflict irreparable damage to human body organs like the central nervous system, peripheral nervous system, lungs, and reproductive and skeletal systems.[9−11] It is worth noting that cadmium has been listed on the red list of priority pollutants by the Department of Environment, United Kingdom, as well as on the black list of the Dangerous Substance Directive in the European Economic Community. Furthermore, the United States Environment Protection Agency has equally grouped cadmium as part of group B1 carcinogens.[12] Hence, there is a great and urgent need to develop an efficient wastewater treatment technology that can remediate water containing cadmium ions.

Several physical and chemical methods have been developed and used to treat water containing Cd(II) ions. They range from ion exchange to precipitation, coagulation/flocculation, membrane filtration, reverse osmosis, solvent extraction, and so forth.[13] However, they suffer major setbacks such as the generation of sludge, high energy consumption, and the formation of other byproducts.[14,15] Adsorption technology has continued to distinguish itself as a suitable technique for the remediation of wastewater contaminated with heavy metal ions because it is cheap, simple to operate, and highly efficient, and its raw materials are readily and abundantly available. Agricultural wastes have continued to gain attention over the years because they are relatively abundant, easily accessible, cost-effective, and reusable. Agricultural wastes, such as papaya seeds,[16] *Quercus robur* acorn caps,[17] *Q. robur* acorn peel,[18] *Quercus coccifera* sawdust,[19] *Lupinus albus* seed hull,[20] pineapple leaf,[21] *Euryale ferox* Salisbury seed coat,[22] banana pseudostem,[23] pine cone,[24] coconut shell,[25] orange peels,[26] macadamia nutshells,[27,28] and *Cedrela odorata* seed waste,[29]

Received: November 4, 2023
Revised: March 28, 2024
Accepted: April 3, 2024
Published: August 30, 2024

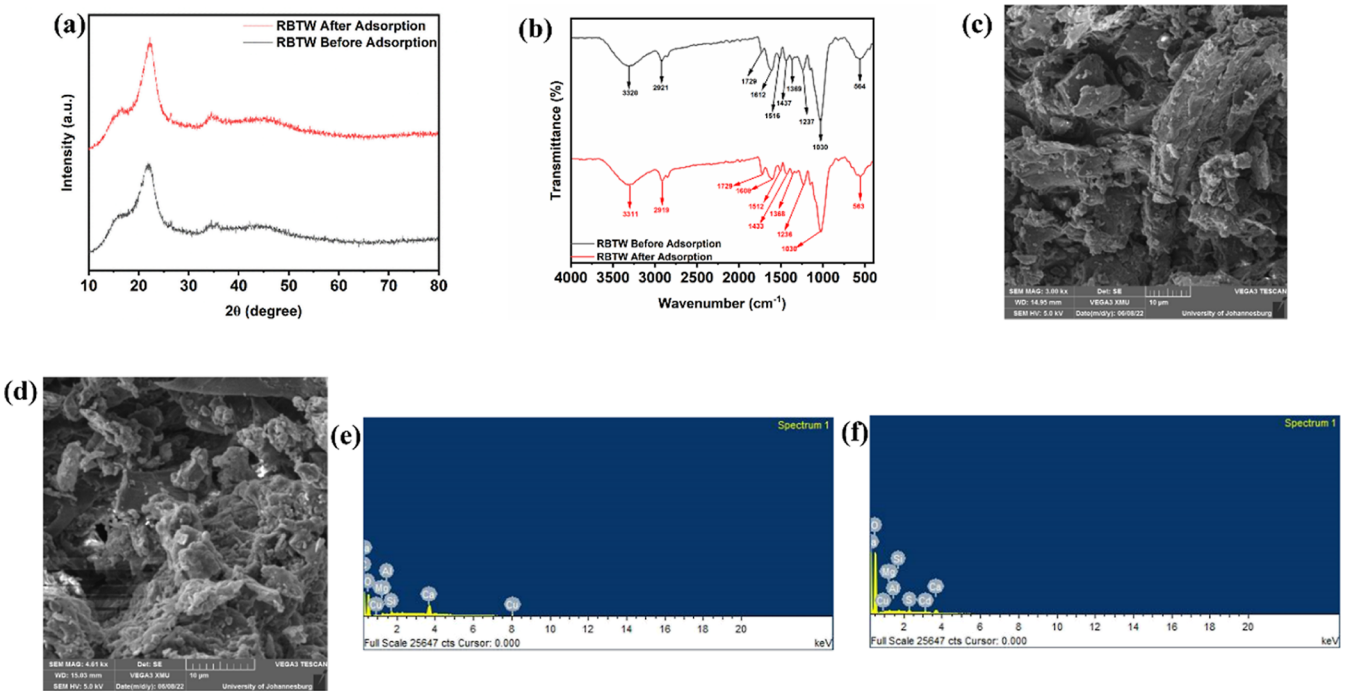

Figure 1. (a) XRD spectra of RBTW before and after adsorption, (b) FTIR spectra of RBTW before and after adsorption, and SEM images of (c) RBTW and (d) RBTW loaded with Cd, and EDX spectra of (e) RBTW and (f) RBTW loaded with Cd.

have been used for wastewater remediation. Rooibos tea waste is cheap, reusable, and simple to prepare and is readily available. In addition, it contains cellulose, lignin, and hemicellulose that serve as binding and active sites for interaction with metal ions. Interestingly, rooibos tea has been successfully applied for the removal of Cr(VI) ions,[30] its shoot has also been employed for the uptake of Cd(II) ions in water.[4] However, it is important to note that when rooibos tea is brewed and consumed, the tea bag is discarded into the environment, and this may lead to environmental pollution. Therefore, we are also eliminating wastes from the environment by harvesting rooibos tea waste for adsorption purposes.

In a bid to turn what is a waste in the environment into a material to remediate the same environment, we have decided to explore the possibility of rooibos tea waste as a suitable and efficient adsorbent material for the removal of cadmium metal ions. Furthermore, to mitigate the general problem of secondary pollution associated with the adsorption process, the spent adsorbent, which is a combination of the rooibos tea waste and the cadmium ions, will be used as a photocatalyst to degrade emerging pharmaceutical pollutants such as sulfamethoxazole. The antibiotic sulfamethoxazole is a widely used drug that belongs to the sulfonamide group.[31] Drugs like this undergo incomplete metabolism in the human body and thus find their way through urine or feces into our water.[32] Sulfamethoxazole has been reported in effluents arising from wastewater treatment plants (0.004−9.460 mg/L),[33] drinking water (60−150 and 10−12 ng/L),[31] and groundwater (1.11 mg/L).[34] Sadly, sulfamethoxazole cannot be sufficiently treated and eliminated by conventional wastewater treatment plants. Therefore, there is a need for total mineralization of sulfamethoxazole, which is why we chose it as our model pollutant. It is important to note that the reuse application of the spent adsorbent for photocatalytic degradation is still in its infant state; hence, through our findings in this work, we shall be contributing to the existing knowledge. To the best of our knowledge, no work has reported the use of rooibos tea waste for the adsorption of Cd(II) ions from an aqueous solution and the reuse of the spent adsorbent as a photocatalyst for the decontamination of water containing sulfamethoxazole.

2. MATERIALS AND METHODS

2.1. Synthesis of Rooibos Tea Waste and Characterization. Rooibos tea waste (RBTW) was harvested and washed in hot water several times until the filtrate obtained from RBTW became clear. Then, RBTW was dried at 80 °C for 48 h. RBTW was then pulverized and sieved to obtain a fine powder with uniform particle size.

The functional groups contained in RBTW were investigated by attenuated total reflectance Fourier transform infrared using a Bruker FTIR Alpha spectrometer (Germany). The amorphous nature of RBTW was examined by X-ray diffractometry (XRD, Rigaku Ultima IV, Japan). Scanning electron microscopy (SEM; TESCAN, Czech Republic) was employed to study the morphology of the adsorbent materials. The elements present were ascertained using energy-dispersive X-ray spectrometry connected to a scanning electron microscope. X-ray photoelectron spectroscopy (XPS) analysis was conducted on a Kratos Axis Ultra device, U.K., with a monochromatic Al Kα radiation. The behavior of the adsorbent in the presence of heat was also studied by thermogravimetry analysis (TGA) Q500 (TA Instruments, USA). The surface area was estimated using a Micrometrics Corporation ASAP 2020 V4.00 surface area and porosity analyzer. The optical properties of the spent adsorbent were analyzed by UV−visible diffusive reflectance spectroscopy (DRS) coupled with a Cary 60 UV−vis spectrophotometer (Malaysia).

2.2. Batch Adsorption Experiments. Batch adsorption studies were conducted to gain more insight into the removal efficiency of RBTW toward the uptake of Cd(II) ions. The effects of solution pH (2−7), RBTW dose (10−500 mg),

https://doi.org/10.1021/acsomega.3c08761
ACS Omega 2024, 9, 38348−38358

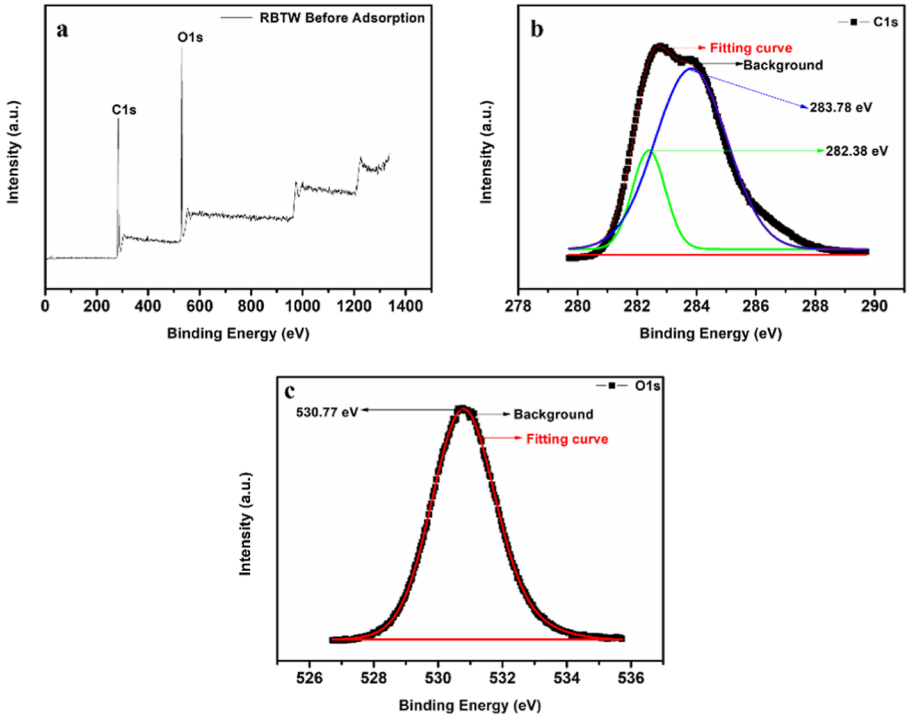

Figure 2. XPS spectra of RBTW before adsorption. Scan survey for (a) RBTW, (b) C 1s, and (c) O 1s.

contact time (5−180 min), Cd(II) ion concentration (10−100 mg/L), and temperature (25−45 °C) were studied. Aliquots were withdrawn and filtered using a syringe membrane (0.22 μm) to remove the adsorbent and the supernatant was analyzed by inductively coupled plasma optical emission spectroscopy. The experiment was carried out in triplicate, and the average of the three results was reported.

2.3. Photocatalytic Degradation Experiment. The spent adsorbent containing a cadmium-loaded RBTW adsorbent was applied toward the degradation of sulfamethoxazole in simulated wastewater. Simply, 50 mg of RBTW-Cd(II) was dispersed into a 50 mL solution of 10 mg/L sulfamethoxazole. The reactor was exposed to both UV and visible light sources. Aliquots were drawn and filtered using a 0.45 μm syringe membrane. The supernatant was analyzed with a UV−visible spectrophotometer (Cary 60 UV−vis, Malaysia), and the degree of mineralization was monitored using total organic carbon (TOC) analyzer (Teledyne Tekmar, USA).

3. RESULTS AND DISCUSSION

3.1. XRD, FTIR, Surface Morphology, Elemental Compositions, and Optical Properties. The XRD patterns obtained before and after the uptake of Cd(II) ions by RBTW are represented in Figure 1a. As expected for an amorphous structure, RBTW showed two peaks at 2θ = 16.25 and 22.19°. In addition, it was observed that the XRD patterns for the cadmium-loaded RBTW showed the same diffraction peaks as the raw RBTW. However, the difference in intensities showed that cadmium ions were adsorbed onto RBTW. The XRD result obtained from this work is similar to previously reported works.[4,35,36]

Figure 1b shows the spectra of RBTW before and after the adsorption of the Cd(II) ions. The peak at 3320 cm^{-1} is indicative of the stretching vibrations of the hydroxyl group.[37] This stretching vibration of the hydroxyl group arises from the lignin, cellulose, and hemicellulose present in RBTW. The band around 2921 cm^{-1} is indicative of asymmetric stretching of C−H vibrations.[30] Also, the band at 1729 cm^{-1} can be indexed to C═O.[38] Furthermore, the bands at 1030 and 564 cm^{-1} can be attributed to the S═O, CH, and CO— bonds.[30] All functional groups identified are consistent with functional groups associated with aspalathin and other related compounds contained in *Aspalathus linearis*.[30] After adsorption, it can be observed that bands such as 3320, 2921, 1729, 1612, 1516, 1437, 1369, 1237, and 564 cm^{-1} moved to 3311, 2919, 1728, 1608, 1512, 1433, 1368, 1236, and 563 cm^{-1}, respectively. This implies that all functional groups such as −OH, CO—, and C−H stretching vibration are likely to be involved in the removal of cadmium ions via hydrogen bonding, electrostatic interaction, and surface complexation.[39,40]

The surface properties of the RBTW adsorbent were probed with SEM. The images obtained from SEM for RBTW are represented in Figure 1c,d. This showed that RBTW contains clusters of particles with pores that serve as available sites for the adsorption of Cd(II) ions (Figure 1c). After the adsorption of cadmium, the SEM image obtained showed the presence of white particles coated on the fibrous surface of the RBTW adsorbent in which the white particles provide evidence that Cd is adsorbed, as confirmed by EDX (Figure 1d). This showed that there was an interaction between RBTW and the cadmium ions. To corroborate this, the EDX spectra before adsorption presented in Figure 1e can be seen showing the presence of elements such as C, O, Cu, Mg, Ca, and Si, which agrees with the elements expected to be present in the raw RBTW. However, after the adsorption of Cd(II) ions, the EDX spectra (Figure 1f) showed the presence of the elements in the raw RBTW as well as Cd. We can therefore state at this point that the presence of cadmium in the spent adsorbent confirmed that there was an interaction between the RBTW adsorbent and the Cd(II) ions in the aqueous solution.

https://doi.org/10.1021/acsomega.3c08761
ACS Omega 2024, 9, 38348−38358

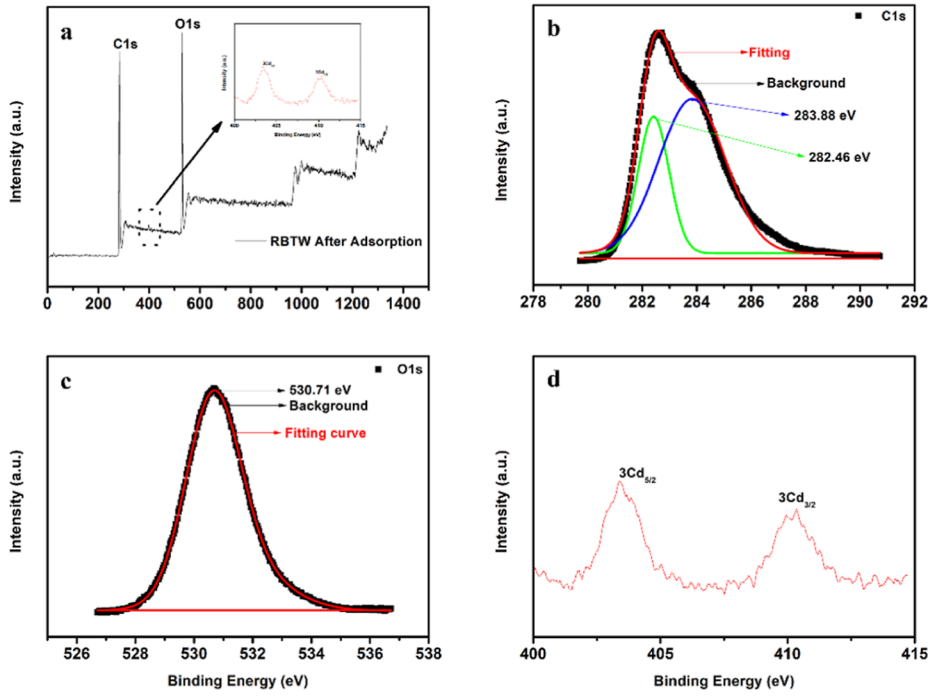

Figure 3. XPS spectra of RBTW after the adsorption of Cd(II). Survey scans for (a) RBTW/Cd^{2+}, (b) C 1s, (c) O 1s, and (d) $3Cd_{5/3}$ and $3Cd_{3/2}$.

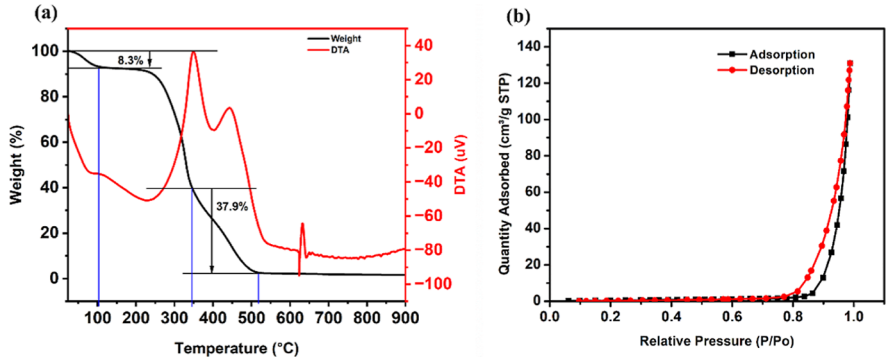

Figure 4. (a) Thermogravimetric thermogram of rooibos tea waste, (b) N_2 adsorption/desorption isotherm of RBTW.

To gain a better understanding of the behavior of RBTW before and after adsorption in the electromagnetic spectrum, UV−vis DRS was used to determine the absorption band edge and band gap. As shown in the Supporting Information, Figure S1a, the raw RBTW absorbed in the visible-light region, while after adsorption of Cd(II) ions, it was seen that the absorption band edge further increased in the visible-light region. This enhancement showed that the presence of Cd(II) ions improved the visible-light harvesting property of RBTW, which, in turn, improved its performance. Similarly, from the Tauc plot (Supporting Information, Figure S1b), the band gap of pristine RBTW reduced from 2.27 to 1.65 eV after adsorption. This implies that less energy would be needed to cause excitation in the presence of light, and this will lead to the production of charge carriers. Overall, both the raw and spent adsorbents are visible-light active, but the spent adsorbent will perform better in the photocatalytic degradation experiment.

3.2. XPS Analysis. To better understand the chemical states of the elements present on the surface of RBTW, XPS analysis was conducted. As illustrated by the survey scan (Figure 2a), RBTW before adsorption showed energy bands indicating the presence of C 1s and O 1s. After deconvoluting the peaks of C 1s (Figure 2b), two peaks resulted at 282.38 and 283.78 eV, which is indicative of a C−C bond. In the same vein, O 1s gave a peak at 530.77 eV, indicative of a C−O bond (Figure 2c).[41]

After adsorption, the band energies of the survey scan showed two extra peaks with energy bands, which can be attributed $3Cd_{5/3}$ and $3Cd_{3/2}$, as shown in Figure 3a,d.[42] Also, there was a shift in the band energies of C 1s (Figure 3b) and O 1s (Figure 3c), showing that there was an interaction between RBTW and Cd(II) ions. The presence of these peaks after removal of Cd(II) ions further established that cadmium was present on the surface of the RBTW adsorbent material.

3.3. Thermogravimetric Analysis and Surface Area. The effect of weight loss and decomposition of RBTW in the presence of heat was studied by exposing it to a temperature between 30 and 900 °C under nitrogen and synthetic air at 10 °C/min. The thermogram represented in Figure 4a indicates that on increasing temperature, RBTW suffered a loss of weight at two different stages. The initial loss in weight of 8.3% occurred between 23 and 102 °C. This initial weight loss can be attributed to the elimination of water molecules as well as

https://doi.org/10.1021/acsomega.3c08761
ACS Omega 2024, 9, 38348−38358

additional volatile compounds present on the RBTW surface.[29,43] The next loss in weight of about 37.8% occurred between 344 and 518 °C. This can be attributed to the elimination of internal constituents such as hemicellulose, cellulose, and lignin.[44,45] It should be noted that above 518 °C, RBTW retained its stability in heat.

The surface area and the estimated textural properties of RBTW were investigated with BET analysis, and the estimated BET value was 2.5108 m^2/g. The N_2 adsorption/desorption isotherm of RBTW at −195.8 °C is represented in Figure 4b. The BJH total pore volume and size were found to be 0.202641 cm^3/g and 22.84 nm, respectively. The surface area and pore volume of RBTW were higher than in the previous report.[46] It is noteworthy that the pore size of RBTW is within 2−50 nm, suggesting the mesoporous nature of the adsorbent.[47]

4. ADSORPTION OF CD(II) IONS USING ROOIBOS TEA WASTE

4.1. Effect of Solution pH. The solution pH plays a critical role in any adsorption reaction as it influences the speciation of the metal ions as well as the charges on the surface of the materials used as an adsorbent.[27,48,49] We investigated the role played by pH in relation to the adsorption capacity of RBTW for the removal of Cd(II) ions by varying the pH between 2 and 7. As depicted in Figure 5a, increasing the pH gave rise to a corresponding increase in the adsorption capacity of RBTW. It was noted that the removal of Cd(II) ions was low in a strongly acidic environment. However, as the pH increases toward the neutral medium, a maximum adsorption capacity of 11.2 mg/g and a removal percentage of 53.49% was attained. From the zeta potential plot (Figure 5b), the point of zero charge of RBTW was 1.11. This implies that RBTW was positively charged when the pH of the solution was lower than 1.11, which means that there was a repulsion between the positively charged surface of the adsorbent and Cd^{2+}, leading to reduced adsorption capacity and removal efficiency. Furthermore, RBTW was negatively charged when the pH was greater than 1.11, thus favoring and aiding the uptake of Cd(II) ions by electrostatic interactions.[12] However, we chose a neutral pH as our optimum pH to work with because similar results reported in past studies confirm that when the pH exceeds 7, the metal ions undergo precipitation.[42]

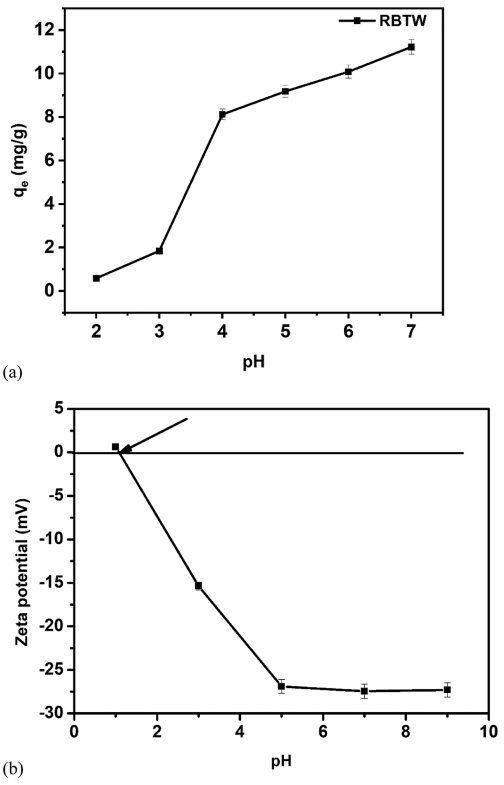

Figure 5. (a) Effect of the solution pH. [Experimental conditions: $[Cd]_0$ = 40 mg/L, adsorbent dose = 100 mg, agitation time = 180 min]; (b) zeta potential of RBTW.

4.2. Effect of Adsorbent Dose. The adsorbent dosage in an adsorption experiment significantly influences the extent to which an adsorbent takes up metal ions in an aqueous solution. It further provides insight into the adsorption capacity of the choice adsorbent for the removal of heavy metals.[50] The influence of RBTW on the uptake of Cd(II) ions was investigated by carrying out an adsorbent dosage study between 10 and 500 mg. As shown in Figure 6, the uptake of Cd(II) ions rose from 15.74 to 84.11% with a corresponding increase in the RBTW dose. This increase can be ascribed to the number of sites available in RBTW for the uptake of Cd(II) ions. However, at a higher adsorbent dose, the surface area of the adsorbent will decrease and the available sites for the uptake of heavy metal ions suffer aggregation. This will result in a decrease in the removal of Cd(II) because both the concentration of the surface metal ions and the concentration of the metal ions in the solution will be at equilibrium.[51] Hence, increasing the adsorbent dosage does not improve the removal of Cd(II) ions. Therefore, the optimum dosage used for further studies in this work is 500 mg.

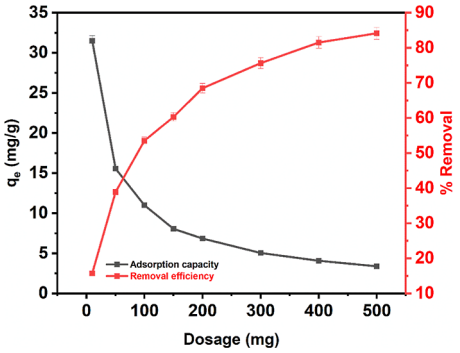

Figure 6. Effect of adsorbent dose [experimental conditions: $[Cd]_0$ = 40 mg/L, pH = 7, agitation time = 180 min].

4.3. Effect of Contact Time. The impact of the contact time between RBTW and Cd(II) ions was evaluated over a time range of 5−180 min. As illustrated in Figure 7, the removal of Cd(II) ions was swift within the first 5 min. This rapid uptake was due to the available unoccupied active sites and pores at the surface of RBTW. This was followed by a slight increase until 60 min as the extent of the Cd(II) ion removal further increased. Thereafter, the adsorption process attained equilibrium between 90 and 180 min. At equilibrium, there was no significant uptake experienced because the available sites present on RBTW have been exhausted. This trend agrees with what has been reported in the literature.[1,4,52]

https://doi.org/10.1021/acsomega.3c08761
ACS Omega 2024, 9, 38348−38358

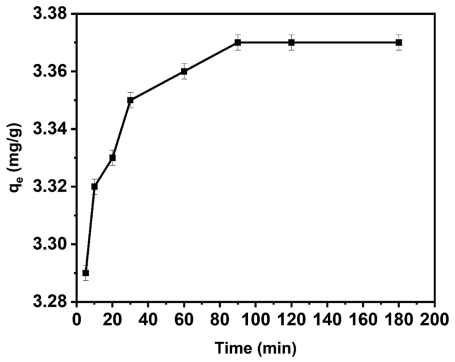

Figure 7. Effect of contact time [experimental conditions: $[Cd]_0$ = 40 mg/L, RBTW dosage = 500 mg, pH = 7, agitation time = 180 min].

4.4. Effect of Initial Cd(II) Ion Concentration and Temperature. The influence of the initial metal ion concentration on the removal of Cd(II) ions using the RBTW adsorbent was investigated by working with a concentration range of 10−100 mg/L at 25, 35, and 45 °C. As shown in Figure 8, it is worth noting that as the temperature

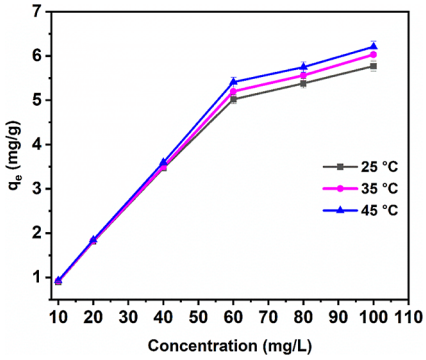

Figure 8. Effect of initial concentration (agitation time = 180 min, RBTW dosage = 500 mg, pH = 7).

increased from room temperature to 45 °C, the adsorption capacity of RBTW toward the uptake of Cd(II) ions increased. This is due to the fact that an increase in temperature causes the average kinetic energy of cadmium ions to gain momentum, which makes them move toward the binding sites of RBTW.[53] Therefore, the number of available binding sites on RBTW is a major factor in the uptake of Cd(II) ions. In addition, an increase in temperature changes the internal structures of RBTW and causes the bonds to become weakened and break. Once this happens, the resistance is weakened, resulting in the movement of the cadmium ions into the readily available pores of RBTW.[47]

4.5. Adsorption Kinetics. To gain a better understanding of the rate at which Cd(II) ions adhere to the RBTW surface, the results obtained were fitted into pseudo-first-order (PFO), pseudo-second-order (PSO) kinetic model, and intraparticle diffusion (IPD) model as linearly expressed in eqs 1−3, respectively

$$\text{PFO: } \ln(q_e - q_t) = \ln q_e - k_1 t \quad (1)$$

$$\text{PSO: } \frac{t}{q_t} = \frac{1}{k_2 q_e^{\,2}} + \frac{t}{q_e} \quad (2)$$

$$\text{IPD: } q_t = k_i t^{1/2} + C \quad (3)$$

Herein, q_e and q_t represent the Cd(II) ions adsorbed at equilibrium and time t, respectively, and these are measured in mg g^{-1}. Also, the rate constants for the PFO kinetic model, k_1, and PSO kinetic model, k_2, are measured in min^{-1} and g mg^{-1} min^{-1} respectively. In addition, k_i represents the IPD rate constant, and it is represented in mg g^{-1} $min^{-1/2}$, while C represents the thickness of the boundary layer.

Table 1 shows the values obtained from the plots of the PFO kinetic plot (Supporting Information, Figure S3a) and PSO

Table 1. Kinetics and Intraparticle Diffusion Model Parameters for the Uptake of Cd(II) by RBTW

Pseudo-First-Order Model	
k_1 (min^{-1})	0.0365
q_e (mg/g)	0.065
R^2	0.9603
Pseudo-Second-Order Model	
k_2 (g mg^{-1} min^{-1})	1.858
q_e (mg/g)	3.37
R^2	1.0000
Intraparticle Diffusion Model	
First Stage	
k_i (mg g^{-1} $min^{-1/2}$)	0.0178
C_i (mg/g)	3.26
R^2	0.89
Second Stage	
k_i (mg g^{-1} $min^{-1/2}$)	0.0009
C_i (mg/g)	3.36
R^2	0.79

kinetic plot (Supporting Information, Figure S3b). The linear regression value (R^2) was found to be greater and unity in the PSO (1.0000) as compared to that in the PFO (0.9603). This implies that the adhesion of Cd(II) ions onto the RBTW adsorbent materials fits more into the PSO kinetic model, and this agrees with chemical adsorption.[54] It further suggests that there is either a sharing or transfer of electrons between RBTW and Cd(II) ions, and Cd(II) is adsorbed by the formation of either a covalent bond or ion exchange.[55] In addition, the rate-controlling steps in the adsorption reaction were investigated by employing the intraparticle diffusion model, as shown in Supporting Information, Figure S3c. According to the literature, the adsorption process is said to be diffusion controlled, provided the plot of q_t vs $t^{1/2}$ is a linear plot. Also, intraparticle diffusion can be said to be the principal adsorption rate-controlling step, provided the plot of q_t vs $t^{1/2}$ passes through the zero origin, but if the plot does not go through the zero origin, then the intraparticle diffusion is not the main adsorption rate-controlling step.[53] As depicted in Supporting Information, Figure S3c, given the fact that the plot was a nonlinear plot that did not pass through the zero origin, it can be deduced that the intraparticle diffusion was not the major adsorption rate-controlling step in the uptake of Cd(II) by RBTW.

4.6. Adsorption Isotherm. In our bid to understand the relationship between the Cd(II) ions and the RBTW adsorbent at different temperatures, we fitted the data obtained from the adsorption process using nonlinear Langmuir, Freundlich, and Temkin models as represented in eqs 4−6, respectively

https://doi.org/10.1021/acsomega.3c08761
ACS Omega 2024, 9, 38348−38358

$$q_e = \frac{q_m K_L C_e}{1 + K_L C_e} \quad (4)$$

$$q_e = K_f C_e^{1/n} \quad (5)$$

$$q_e = B \ln(A_T C_e) \quad (6)$$

where q_m (mg/g), b (L/mg), K_F (mg/g), n, A_T (L/mg), b_T (J/mol), T (K), and R (8.314 J/mol/K) represent the maximum adsorption capacity, the free energy of adsorption, Freundlich constant related to adsorption capacity, adsorption intensity, equilibrium binding constant related to the maximum binding energy, Temkin isotherm constant corresponding to the heat of adsorption, absolute temperature, and universal gas constant, respectively.

The values deduced from the fitted plots and the correlation factor are shown in Table 2. The adsorption of Cd(II) by RBTW favored the Langmuir isotherm model because of the highest R^2 values obtained.

Table 2. Adsorption Parameters for Cd(II) onto RBTW Adsorbent

isotherm model	temperature (K)		
	298	308	318
Langmuir			
q_{max} (mg/g)	6.68	6.97	7.13
K_L (L/mg)	0.16	0.17	0.20
R^2	0.9905	0.9869	0.9783
Freundlich			
N	2.69	2.69	2.80
K_F (mg/g)	1.53	1.62	1.80
R^2	0.9089	0.9071	0.8803
Temkin			
A_T (L/mg)	1.66	1.78	2.03
b_T (kJ/mol)	1.41	1.46	1.49
R^2	0.9782	0.9744	0.9601

The dimensionless factor (R_L) expressed with eq 7 is important in gaining a better understanding of the feasibility of the adsorption process

$$R_L = \frac{1}{1 + K_L C_0} \quad (7)$$

K_L provides insight into the bonding of the adsorbent surface for the solute ions, while C_0 is the initial Cd(II) concentration. The uptake of Cd(II) ions by RBTW is said to be possible when R_L is between 0 and 1. In our study, the R_L values for the three temperatures investigated were below 1. This indicates the possibility of using RBTW to remove Cd(II). We also compared the adsorption capacity of Cd(II) by RBTW used in this work with other adsorbents, as shown in Table 3 and this showed that RBTW possessed a better adsorption capacity.

4.7. Adsorption Thermodynamics. The thermodynamic principles that control the removal of Cd(II) ions by RBTW were better understood by the values of $\Delta G°$, $\Delta H°$, and $\Delta S°$ by using eqs 8 and 9

$$\Delta G° = -RT \ln K_c \quad (8)$$

Table 3. Comparing the Adsorption Capacity of Cd(II) by RBTW with Other Adsorbents

adsorbent	adsorption capacity (mg/g)	references
corn cob	5.09	56
poplar branches	2.10	57
hazelnut shell	5.42	58
bagasse fly ash	6.19	59
oak bark char	5.40	60
wheat bran	0.70	61
phragmites biomass	6.40	62
sawdust	5.37	63
bagasse fly ash	2.00	64
RBTW	7.13	this work

$$\ln K_c = \frac{\Delta S°}{R} - \frac{\Delta H°}{RT} = m\frac{q_e}{C_e} \quad (9)$$

Here, R is the universal gas constant in J/mol/K, T is the temperature in K, and K_c represents the equilibrium constant. Also, $\Delta G°$, $\Delta H°$, and $\Delta S°$ represent the changes in Gibbs free energy, enthalpy, and entropy, respectively. The values for the enthalpy and entropy change were obtained from a plot of ln K_c against $1/T$ as depicted in Supporting Information, Figure S4. As represented in Table 4, the adsorption of Cd(II) ions by RBTW is endothermic, as well as spontaneous. Also, the extent of disorder at the interface of RBTW and Cd(II) increased.

Table 4. Thermodynamic Data for Cd(II) onto RBTW Adsorbent

temperature (°C)	$\Delta G°$ (kJ/mol)	$\Delta H°$ (kJ/mol)	$\Delta S°$ (kJ/mol/K)
25	−319.48	+8.216	+0.012
35	−365.92		
45	−406.88		

4.8. Influence of Coexisting Ions. It is well-known that numerous metal ions exist in wastewater and natural water. Therefore, in this study, we further went ahead to probe into what happens when Ni^{2+} and Cu^{2+} coexist with Cd^{2+} in wastewater. Supporting Information, Figure S5, shows the adhesion of Ni^{2+}, Cu^{2+}, and Cd^{2+} ions on the RBTW adsorbent. In Cd^{2+} ion adsorption, Ni^{2+} and Cu^{2+} were inequitable with Ni^{2+} ion, having the better effect on increasing from 10 to 150 mg/L, thereby causing a reduction in Cd^{2+} ion adsorption from 80 to 26 percent removal. Therefore, the order of interference was $Ni^{2+} > Cu^{2+}$, which is connected to the Z/R value of cations Ni^{2+} (2/0.70 nm) and Cu^{2+} (2/0.73 nm). From the result, Cd^{2+} (2/0.154 nm) ions were less adsorbed because of repulsion forces produced with higher electron affinity to Cu^{2+}.[65]

4.9. Adsorption Mechanism. As reported earlier, the adsorption kinetics revealed that the rate at which Cd(II) ions adhered to RBTW fits more into the pseudo-second-order kinetic model. This implies that the available sites of RBTW and the Cd(II) ions in the solution controlled the mechanism of the chemical interaction that existed between the Cd(II) ions and the RBTW adsorbent. We can therefore infer that there was a possibility of an interaction between the Cd(II) ions and the functional groups available on the surface of the adsorbent. The FTIR spectra represented in Figure 1b confirmed all functional groups present in RBTW before and after the removal of Cd(II) ions. The shifts in the peaks after

https://doi.org/10.1021/acsomega.3c08761
ACS Omega 2024, 9, 38348−38358

adsorption further substantiate our inference that there was an interaction between the functional groups and the Cd(II) ions. For example, the O−H_{str} vibration band moved from 3320 to 3311 cm^{-1}. This is indicative of hydrogen bonding between the Cd(II) and the −OH groups of RBTW.[39] Again, since all of the major peaks shifted, it further corroborated the fact that there was indeed a reaction between the Cd(II) ions and RBTW. In addition, the SEM images with and without cadmium showed that the pores available in the raw RBTW were filled by the Cd(II) ions after adsorption (Figure 1c,d). Furthermore, EDX (Figure 1e,f) validates the presence of Cd(II) ions in the spent RBTW. The XPS spectra of RBTW after adsorption showed that the energy bands of C 1s increased (Figure 3b), while those of O 1s reduced (Figure 3c). Also, additional peaks of $Cd_{5/2}$ and $Cd_{3/2}$ (Figure 3d) are indicative of cadmium appearing after adsorption. This indeed confirms the presence of cadmium in RBTW after adsorption as well as the oxidation state of cadmium as Cd^{2+} in the RWBT/Cd^{2+} spent adsorbent. In summary, the adsorption pathway illustrating the adhesion of Cd(II) ions to the surface of RBTW is shown in Figure 9.

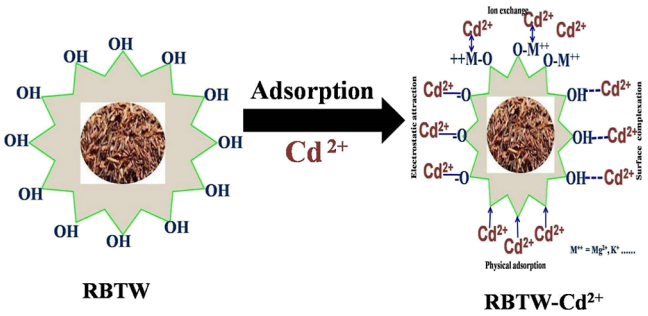

Figure 9. Adsorption mechanism showing the interaction between Cd(II) ions and RBTW.

5. PHOTOCATALYTIC DEGRADATION OF SULFAMETHOXAZOLE USING CD(II) SPENT ADSORBENT

Adsorption is known to promote secondary pollution by the generation of a spent adsorbent. Therefore, in a bid to mitigate this, we used the Cd(II) spent adsorbent as a photocatalyst under a UV lamp and visible light for the degradation of sulfamethoxazole. As shown in Supporting Information Figure S6, the reaction was left to equilibrate in the dark for 30 min before the irradiation. In the presence of a UV lamp, the extent of sulfamethoxazole degradation was found to be 53.2% after 150 min. However, under visible light, the extent of the breakdown increased to 69%. This increase showed that the RBTW-Cd(II) spent adsorbent absorbs more in the visible-light region, thereby resulting in the generation of photogenerated charge carriers that significantly took part in the degradation of sulfamethoxazole. When the RBTW/Cd(II) spent adsorbent is irradiated, electrons are ejected from the valence band and enter the conduction band, leaving a photogenerated hole at the valence band. The photogenerated holes are a strong oxidant that can react directly with the sulfamethoxazole to break it down. The holes can also react with water molecules to produce hydroxyl radicals, which also take part in the degradation process. Similarly, the photogenerated electrons react with dissolved oxygen to produce superoxide. The complementary effects of the oxidants and highly reactive radicals promote the extent of degradation of sulfamethoxazole. The possible reaction mechanism is shown in Figure 10.[66] We also compared the removal performance of the spent adsorbent with other catalysts in the degradation of pharmaceuticals, as shown in Supporting Information, Table S1.

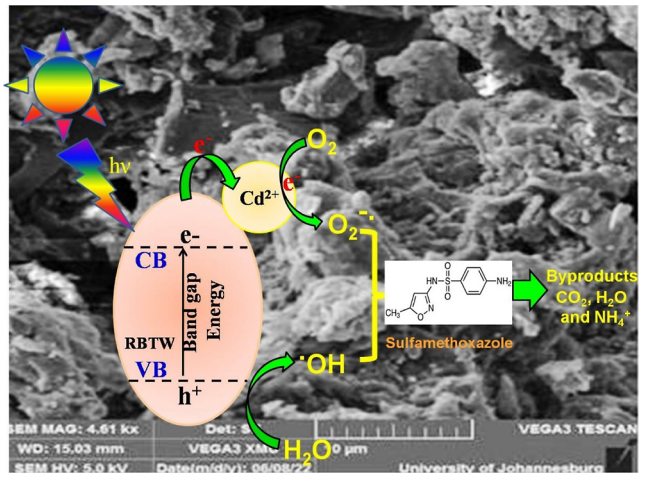

Figure 10. Mechanism of sulfamethoxazole degradation.

The apparent rate constant under the UV and visible-light sources was deduced by analyzing the data using the PFO kinetic model as reported in eq 10

$$\ln C_0/C_t = kt \quad (10)$$

From the results obtained, the degradation of sulfamethoxazole using the spent adsorbent was faster in the presence of visible light (0.01020 min^{-1}) than in the UV lamp (0.00698 min^{-1}). The degree of mineralization as obtained from the TOC content was 53%. This result further validates the efficiency and suitability of RBTW/Cd(II) for photocatalytic abatement of pharmaceutical contaminants in water. It equally shows that the reuse application of spent adsorbent as a catalyst for the photocatalytic degradation of sulfamethoxazole offers a viable alternative in alleviating the problem of secondary pollution, which is commonly associated with adsorption technology.

6. CONCLUSIONS

Overall, we successfully prepared, characterized, and applied a cheap, readily available, and efficient adsorbent material, rooibos tea waste (RBTW) for the removal of Cd(II) ions and reused it for the photocatalytic degradation of sulfamethoxazole. The synthesized RBTW exhibited a satisfactory adsorption capacity and efficiency of 7.13 mg/g and 90.63%, respectively, for 10 mg/L Cd(II) ions at 45 °C, 180 min agitation time, pH 7, and dosage of 500 mg. The uptake of Cd(II) ions by RBTW was well fitted by the pseudo-second-order kinetic model and best described by the Langmuir isotherm. Furthermore, the cadmium-loaded adsorbent successfully degraded 69% of 10 mg/L sulfamethoxazole within 150 min by using visible light. The degree of mineralization from the TOC data showed that 53% of sulfamethoxazole was mineralized by the spent adsorbent. Thermodynamically, the adsorption process was endothermic as well as spontaneous. Also, this study has given the proof of

https://doi.org/10.1021/acsomega.3c08761
ACS Omega 2024, 9, 38348−38358

concept that the rooibos adsorbent can successfully retain cadmium and that the cadmium-loaded adsorbent can be reused for photocatalysis. It is acknowledged that it has paved the way for some future work to check the life span of the catalyst and how to reuse the catalyst once it has become spent. In general, due to the satisfactory performance of RBTW in the remediation of Cd(II) ions and the efficient performance of the spent adsorbent in the breakdown of sulfamethoxazole, RBTW lends itself as a suitable material for the treatment of wastewater polluted with other heavy metals and to be reused to prevent secondary pollution, which is a major setback of adsorption technology.

■ ASSOCIATED CONTENT

Supporting Information

The Supporting Information is available free of charge at https://pubs.acs.org/doi/10.1021/acsomega.3c08761.

UV−vis DRS spectra of RBTW before and after adsorption, Tauc plot of RBTW before and after adsorption, pore diameter of RBTW, PFO and PSO kinetic models, Weber−Morris intraparticle diffusion model, plot of ln K_c versus $1/T$, effect of coexisting ions, photocatalytic degradation plot of sulfamethoxazole using RBTW/Cd(II) spent adsorbent in the presence of a UV lamp and visible light, and comparison of the removal performance of RBTW/Cd(II) spent adsorbent with other catalysts in the degradation of pharmaceuticals (PDF)

■ AUTHOR INFORMATION

Corresponding Author

Kriveshini Pillay − *Department of Chemical Sciences, University of Johannesburg, Doornfontein 2028, South Africa;* orcid.org/0000-0002-2134-7666; Email: kriveshinip@uj.ac.za

Author

Opeoluwa I. Adeiga − *Department of Chemical Sciences, University of Johannesburg, Doornfontein 2028, South Africa*

Complete contact information is available at: https://pubs.acs.org/10.1021/acsomega.3c08761

Notes

The authors declare no competing financial interest.

■ ACKNOWLEDGMENTS

The authors acknowledge the Faculty of Science and the Department of Chemical Sciences, University of Johannesburg. Also, the authors would like to appreciate the National Research Foundation (NRF) of South Africa.

■ REFERENCES

(1) Thabede, P. M.; Shooto, N. D.; Xaba, T.; Naidoo, E. B. Adsorption studies of toxic cadmium (II) and chromium (VI) ions from aqueous solution by activated black cumin (Nigella sativa) seeds. *J. Environ. Chem. Eng.* **2020**, *8* (4), 104045.

(2) Alqadami, A. A.; Naushad, M.; Abdalla, M. A.; Ahamad, T.; Abdullah ALOthman, Z.; Alshehri, S. M.; Ghfar, A. A. Efficient removal of toxic metal ions from wastewater using a recyclable nanocomposite: a study of adsorption parameters and interaction mechanism. *J. Clean. Prod.* **2017**, *156*, 426−436.

(3) da Silva, T. L.; da Silva, A. C.; Vieira, M. G. A.; Gimenes, M. L.; da Silva, M. G. C. Biosorption study of copper and zinc by particles produced from silk sericin-alginate blend: evaluation of blend proportion and thermal cross-linking process in particles production. *J. Clean. Prod.* **2016**, *137*, 1470−1478.

(4) Kanu, S. A.; Moyo, M.; Khamlich, S.; Okonkwo, J. O. Adsorption of cadmium from aqueous solution using Rooibos shoots as adsorbent. *Toxicol. Environ. Chem.* **2014**, *96* (10), 1452−1462.

(5) Zeng, L.; Gong, J.; Rong, P.; Liu, C.; Chen, J. A portable and quantitative biosensor for cadmium detection using glucometer as the point-of-use device. *Talanta* **2019**, *198*, 412−416.

(6) Goering, P.; Waalkes, M.; Klaassen, C. Toxicology of cadmium. *Toxicology of Metals: Biochemical Aspects*; Springer, 1995; pp 189−214.

(7) Wang, C.; Wang, B.; Liu, J.; Yu, L.; Sun, H.; Wu, J. Adsorption of Cd (II) from acidic aqueous solutions by tourmaline as a novel material. *Chin. Sci. Bull.* **2012**, *57*, 3218−3225.

(8) Waisberg, M.; Joseph, P.; Hale, B.; Beyersmann, D. Molecular and cellular mechanisms of cadmium carcinogenesis. *Toxicology* **2003**, *192* (2−3), 95−117.

(9) Yang, T.; Sheng, L.; Wang, Y.; Wyckoff, K. N.; He, C.; He, Q. Characteristics of cadmium sorption by heat-activated red mud in aqueous solution. *Sci. Rep.* **2018**, *8* (1), 13558.

(10) Rahimzadeh, M. R.; Rahimzadeh, M. R.; Kazemi, S.; Moghadamnia, A.-a. Cadmium toxicity and treatment: An update. *Caspian J. Intern. Med.* **2017**, *8* (3), 135.

(11) Kellen, E.; Zeegers, M. P.; Hond, E. D.; Buntinx, F. Blood cadmium may be associated with bladder carcinogenesis: the Belgian case-control study on bladder cancer. *Cancer Detect. Prev.* **2007**, *31* (1), 77−82.

(12) Wang, F. Y.; Wang, H.; Ma, J. W. Adsorption of cadmium (II) ions from aqueous solution by a new low-cost adsorbent—Bamboo charcoal. *J. Hazard. Mater.* **2010**, *177* (1−3), 300−306.

(13) Haris, M. R. H. M.; Wahab, N. A. A.; Reng, C. W.; Azahari, B.; Sathasivam, K. The sorption of cadmium (II) ions on mercerized rice husk and activated carbon. *Turk. J. Chem.* **2011**, *35* (6), 939−950.

(14) Rao, K.; Mohapatra, M.; Anand, S.; Venkateswarlu, P. Review on cadmium removal from aqueous solutions. *Int. J. Eng. Sci. Technol.* **2011**, *2*(7).

(15) Naeem, M. A.; Imran, M.; Amjad, M.; Abbas, G.; Tahir, M.; Murtaza, B.; Zakir, A.; Shahid, M.; Bulgariu, L.; Ahmad, I. Batch and column scale removal of cadmium from water using raw and acid activated wheat straw biochar. *Water* **2019**, *11* (7), 1438.

(16) Shooto, N.; Naidoo, E. Detoxification of wastewater by paw-paw (carica papaya L.) seeds adsorbents. *Asian J. Chem.* **2019**, *31* (10), 2249−2256.

(17) Zeybek, Z.; Dursun, S. Investigation of Copper removal mechanisms on Quercus robur acorn caps: Equilibrium, kinetics, thermodynamic and characterization studies. *Appl. Water Sci.* **2021**, *11* (6), 104.

(18) Kuppusamy, S.; Venkateswarlu, K.; Thavamani, P.; Lee, Y. B.; Naidu, R.; Megharaj, M. Quercus robur acorn peel as a novel coagulating adsorbent for cationic dye removal from aquatic ecosystems. *Ecol. Eng.* **2017**, *101*, 3−8.

(19) Argun, M. E.; Dursun, S.; Ozdemir, C.; Karatas, M. Heavy metal adsorption by modified oak sawdust: Thermodynamics and kinetics. *J. Hazard. Mater.* **2007**, *141* (1), 77−85.

(20) Abdel Hafez, A. A.; Abd-Rabboh, H. S.; Al-Marri, A. M.; Aboterika, A. H. Removal of Toxic Lead from Wastewater by Lupinus albus Seed Hull. *ACS Omega* **2023**, *8*, 42622−42631.

(21) Srikhaow, A.; Win, E. E.; Amornsakchai, T.; Kiatsiriroat, T.; Kajitvichyanukul, P.; Smith, S. M. Biochar Derived from Pineapple Leaf Non-Fibrous Materials and Its Adsorption Capability for Pesticides. *ACS Omega* **2023**, *8* (29), 26147−26157.

(22) Devi, B.; Goswami, M.; Rabha, S.; Kalita, S.; Sarma, H. P.; Devi, A. Efficacious Sorption Capacities for Pb (II) from Contaminated Water: A Comparative Study Using Biowaste and Its Activated Carbon as Potential Adsorbents. *ACS Omega* **2023**, *8* (17), 15141−15151.

(23) Kumar, P.; Reddy, S. N. In Situ Encapsulation of Nanometals in Carbon Matrix from Hazardous Wastewater with Cogeneration of H2

Using Banana Pseudostem. *Ind. Eng. Chem. Res.* **2023**, *62*, 10358−10371.
(24) Dawood, S.; Sen, T. K.; Phan, C. Synthesis and characterization of slow pyrolysis pine cone bio-char in the removal of organic and inorganic pollutants from aqueous solution by adsorption: kinetic, equilibrium, mechanism and thermodynamic. *Bioresour. Technol.* **2017**, *246*, 76−81.
(25) Zhao, X.; Zeng, X.; Qin, Y.; Li, X.; Zhu, T.; Tang, X. An experimental and theoretical study of the adsorption removal of toluene and chlorobenzene on coconut shell derived carbon. *Chemosphere* **2018**, *206*, 285−292.
(26) Safari, E.; Rahemi, N.; Kahforoushan, D.; Allahyari, S. Copper adsorptive removal from aqueous solution by orange peel residue carbon nanoparticles synthesized by combustion method using response surface methodology. *J. Environ. Chem. Eng.* **2019**, *7* (1), 102847.
(27) Adeiga, O. I.; Velempini, T.; Pillay, K. Polyaniline-decorated macadamia nutshell composite: An adsorbent for the removal of highly toxic Cr (VI) and efficient catalytic activity of the spent adsorbent for reuse. *Polym. Bull.* **2023**, *80* (2), 1951−1973.
(28) Omo-Okoro, P.; Adeiga, O.; Velempini, T.; Prabakaran, E.; Curtis, C.; Pillay, K. Nickel ion removal from aqueous media using polyaniline-macadamia nutshells and its reuse for photodegradation of orange dye. *Int. J. Environ. Sci. Technol.* **2023**, *20* (8), 8655−8672.
(29) Babalola, J. O.; Koiki, B. A.; Eniayewu, Y.; Salimonu, A.; Olowoyo, J. O.; Oninla, V. O.; Alabi, H. A.; Ofomaja, A. E.; Omorogie, M. O. Adsorption efficacy of Cedrela odorata seed waste for dyes: non linear fractal kinetics and non linear equilibrium studies. *J. Environ. Chem. Eng.* **2016**, *4* (3), 3527−3536.
(30) Çelebi, H. Recovery of detox tea wastes: usage as a lignocellulosic adsorbent in Cr6+ adsorption. *J. Environ. Chem. Eng.* **2020**, *8* (5), 104310.
(31) Kumar, A.; Kumar, A.; Sharma, G.; Al-Muhtaseb, A. H.; Naushad, M.; Ghfar, A. A.; Stadler, F. J. Quaternary magnetic BiOCl/g-C3N4/Cu2O/Fe3O4 nano-junction for visible light and solar powered degradation of sulfamethoxazole from aqueous environment. *Chem. Eng. J.* **2018**, *334*, 462−478.
(32) Zhu, W.; Sun, F.; Goei, R.; Zhou, Y. Facile fabrication of RGO-WO3 composites for effective visible light photocatalytic degradation of sulfamethoxazole. *Appl. Catal., B* **2017**, *207*, 93−102.
(33) Mafa, P. J.; Kuvarega, A. T.; Mamba, B. B.; Ntsendwana, B. Photoelectrocatalytic degradation of sulfamethoxazole on g-C3N4/BiOI/EG pn heterojunction photoanode under visible light irradiation. *Appl. Surf. Sci.* **2019**, *483*, 506−520.
(34) Su, T.; Deng, H.; Benskin, J. P.; Radke, M. Biodegradation of sulfamethoxazole photo-transformation products in a water/sediment test. *Chemosphere* **2016**, *148*, 518−525.
(35) Sharma, G.; Naushad, M. Adsorptive removal of noxious cadmium ions from aqueous medium using activated carbon/zirconium oxide composite: Isotherm and kinetic modelling. *J. Mol. Liq.* **2020**, *310*, 113025.
(36) Moyo, M.; Chikazaza, L.; Nyamunda, B. C.; Guyo, U. Adsorption batch studies on the removal of Pb (II) using maize tassel based activated carbon. *J. Chem.* **2013**, *2013*, 1−8.
(37) De Goes Sampaio, C.; Silva, J. G. A. E.; De Brito, E. S.; Becker, H.; Trevisan, M. T. S.; Owen, R. W. Chromium (VI) remediation in aqueous solution by waste products (peel and seed) of mango (Mangifera indica L.) cultivars. *Environ. Sci. Pollut. Res.* **2019**, *26*, 5588−5600.
(38) Tejada-Tovar, C.; Herrera-Barros, A.; Villabona-Ortíz, A. Assessment of chemically modified lignocellulose waste for the adsorption of Cr (VI). *Rev. Fac. Ing.* **2020**, *29* (54), No. e10298.
(39) Siddiqui, S. I.; Chaudhry, S. A. Nanohybrid composite Fe2O3-ZrO2/BC for inhibiting the growth of bacteria and adsorptive removal of arsenic and dyes from water. *J. Clean. Prod.* **2019**, *223*, 849−868.
(40) Liu, L.; Fan, S.; Li, Y. Removal behavior of methylene blue from aqueous solution by tea waste: kinetics, isotherms and mechanism. *Int. J. Environ. Res. Publ. Health* **2018**, *15* (7), 1321.
(41) Wu, Y.; Lin, Y.; Xu, J. Synthesis of Ag-Ho, Ag-Sm, Ag-Zn, Ag-Cu, Ag-Cs, Ag-Zr, Ag-Er, Ag-Y and Ag-Co metal organic nanoparticles for UV-Vis-NIR wide-range bio-tissue imaging. *Photochem. Photobiol. Sci.* **2019**, *18*, 1081−1091.
(42) Umejuru, E. C.; Prabakaran, E.; Pillay, K. Coal fly ash coated with carbon hybrid nanocomposite for remediation of cadmium (II) and photocatalytic application of the spent adsorbent for reuse. *Results Mater.* **2020**, *7*, 100117.
(43) Ali, Z.; Sajid, M.; Raza, N.; Sohail, Y.; Hayat, M.; Manzoor, S.; Shakeel, N.; Aziz Gill, K.; Ifseisi, A. A.; Zahid Ansari, M. Study of modified biomass of Gossypium hirsutum as heavy metal biosorbent. *Arab. J. Chem.* **2023**, *16* (12), 105332.
(44) Putri, K. N. A.; Kaewpichai, S.; Keereerak, A.; Chinpa, W. Facile green preparation of lignocellulosic biosorbent from lemongrass leaf for cationic dye adsorption. *J. Polym. Environ.* **2021**, *29*, 1681−1693.
(45) Sera, P. R.; Diagboya, P. N.; Akpotu, S. O.; Mtunzi, F. M.; Chokwe, T. B. Potential of valourized Moringa oleifera seed waste modified with activated carbon for toxic metals decontamination in conventional water treatment. *Bioresour. Technol. Rep.* **2021**, *16*, 100881.
(46) Joshi, S.; Kataria, N.; Garg, V.; Kadirvelu, K. Pb2+ and Cd2+ recovery from water using residual tea waste and SiO2@ TW nanocomposites. *Chemosphere* **2020**, *257*, 127277.
(47) Zhou, C.; Han, C.; Min, X.; Yang, T. Effect of different sulfur precursors on efficient chromium (VI) removal by ZSM-5 zeolite supporting sulfide nano zero-valent iron. *Chem. Eng. J.* **2022**, *427*, 131515.
(48) Daraei, H.; Mittal, A.; Noorisepehr, M.; Daraei, F. Kinetic and equilibrium studies of adsorptive removal of phenol onto eggshell waste. *Environ. Sci. Pollut. Res.* **2013**, *20*, 4603−4611.
(49) Guyo, U.; Mhonyera, J.; Moyo, M. Pb (II) adsorption from aqueous solutions by raw and treated biomass of maize stover-a comparative study. *Process Saf. Environ. Prot.* **2015**, *93*, 192−200.
(50) Moafi, H.; Ansari, R.; Ostovar, F. Ag2O/Sawdust nanocomposite as an efficient adsorbent for removal of hexavalent chromium ions from aqueous solutions. *J. Mater. Environ. Sci.* **2016**, *7* (6), 2051−2068.
(51) Naiya, T. K.; Bhattacharya, A. K.; Das, S. K. Adsorption of Cd (II) and Pb (II) from aqueous solutions on activated alumina. *J. Colloid Interface Sci.* **2009**, *333* (1), 14−26.
(52) Xu, Z.; Huang, W.; Xie, H.; Feng, X.; Wang, S.; Song, H.; Xiong, J.; Mailhot, G. Co-adsorption and interaction mechanism of cadmium and sulfamethazine onto activated carbon surface. *Colloids Surf. A Physicochem. Eng. Asp.* **2021**, *619*, 126540.
(53) Qiu, R.; Cheng, F.; Huang, H. Removal of Cd2+ from aqueous solution using hydrothermally modified circulating fluidized bed fly ash resulting from coal gangue power plant. *J. Clean. Prod.* **2018**, *172*, 1918−1927.
(54) Lei, T.; Li, S.-J.; Jiang, F.; Ren, Z.-X.; Wang, L.-L.; Yang, X.-J.; Tang, L.-H.; Wang, S.-X. Adsorption of cadmium ions from an aqueous solution on a highly stable dopamine-modified magnetic nano-adsorbent. *Nanoscale Res. Lett.* **2019**, *14*, 352−417.
(55) Ho, Y.-S. Review of second-order models for adsorption systems. *J. Hazard. Mater.* **2006**, *136* (3), 681−689.
(56) Leyva-Ramos, R.; Bernal-Jacome, L.; Acosta-Rodriguez, I. Adsorption of cadmium (II) from aqueous solution on natural and oxidized corncob. *Sep. Purif. Technol.* **2005**, *45* (1), 41−49.
(57) Al-Masri, M.; Amin, Y.; Al-Akel, B.; Al-Naama, T. Biosorption of cadmium, lead, and uranium by powder of poplar leaves and branches. *Appl. Biochem. Biotechnol.* **2010**, *160*, 976−987.
(58) Bulut, Y.; Tez, Z. Adsorption studies on ground shells of hazelnut and almond. *J. Hazard. Mater.* **2007**, *149* (1), 35−41.
(59) Srivastava, V. C.; Mall, I. D.; Mishra, I. M. Adsorption of toxic metal ions onto activated carbon: Study of sorption behaviour through characterization and kinetics. *Chem. Eng. Process.* **2008**, *47* (8), 1269−1280.
(60) Mohan, D.; Pittman, C. U.; Bricka, M.; Smith, F.; Yancey, B.; Mohammad, J.; Steele, P. H.; Alexandre-Franco, M. F.; Gómez-

https://doi.org/10.1021/acsomega.3c08761
ACS Omega 2024, 9, 38348−38358

Serrano, V.; Gong, H. Sorption of arsenic, cadmium, and lead by chars produced from fast pyrolysis of wood and bark during bio-oil production. *J. Colloid Interface Sci.* **2007**, *310* (1), 57−73.
(61) Singh, K.; Singh, A.; Hasan, S. Low cost bio-sorbent 'wheat bran'for the removal of cadmium from wastewater: kinetic and equilibrium studies. *Bioresour. Technol.* **2006**, *97* (8), 994−1001.
(62) Amro, A. N.; Abhary, M. K.; Shaikh, M. M.; Ali, S. Removal of lead and cadmium ions from aqueous solution by adsorption on a low-cost phragmites biomass. *Processes* **2019**, *7* (7), 406.
(63) Bulut, Y.; Tez, Z. Removal of heavy metals from aqueous solution by sawdust adsorption. *J. Environ. Sci.* **2007**, *19* (2), 160−166.
(64) Gupta, V. K.; Jain, C. K.; Ali, I.; Sharma, M.; Saini, V. Removal of cadmium and nickel from wastewater using bagasse fly ash—a sugar industry waste. *Water Res.* **2003**, *37* (16), 4038−4044.
(65) Fouda-Mbanga, B.; Prabakaran, E.; Pillay, K. Cd2+ ion adsorption and re-use of spent adsorbent with N-doped carbon nanoparticles coated on cerium oxide nanorods nanocomposite for fingerprint detection. *Chem. Phys. Impact* **2022**, *5*, 100083.
(66) Paragas, L. K. B.; de Luna, M. D. G.; Doong, R.-A. Rapid removal of sulfamethoxazole from simulated water matrix by visible-light responsive iodine and potassium co-doped graphitic carbon nitride photocatalysts. *Chemosphere* **2018**, *210*, 1099−1107.

https://doi.org/10.1021/acsomega.3c08761
ACS Omega 2024, 9, 38348−38358